POWER SPECTRA OF BLACK HOLES AND NEUTRON STARS AS A PROBE OF HYDRODYNAMICAL STRUCTURE OF THE SOURCE: DIFFUSION THEORY AND ITS APPLICATION TO X-RAY OBSERVATIONS

Lev Titarchuk[1], **Nikolai Shaposhnikov**[2], **and Vadim Arefiev**[3]

[1]*George Mason University/Center for Earth Observing and Space Research, Fairfax, VA 22030; US Naval Research Laboratory, Code 7655, Washington, DC 20375-5352; ltitarchuk@ssd5.nrl.navy.mil;*
[2]*Goddard Space Flight Center, NASA/Universities Space Research Association, code 662, Greenbelt MD 20771; nikolai@milkyway.gsfc.nasa.gov*
[3]*Space Research Institute (IKI), Russian Academy of Science, Profsoyuznaya 84/32, 117997, Moscow, Russia, gita@hea.iki.rssi.ru*

ABSTRACT

We present a model of Fourier Power Density Spectrum (PDS) formation in accretion powered X-ray binary systems derived from the first principles of the diffusion theory. Timing properties of X-ray emission are considered to be a result of diffusive propagation of the driving perturbations in a bounded medium. We prove that the integrated power of the resulting PDS, P_x is only a small fraction of the integrated power of the driving oscillations, P_{dr} which is distributed over the disk. Furthermore, we demonstrate that the power P_x is inversely proportional to the characteristic frequency of the driving oscillations ν_{dr} which is likely scaled with the frequency of the local gravity waves in the disk (Keplerian frequency). Keeping in mind that ν_{dr} increases towards soft states leads us to conclude that the power P_x declines towards soft states. This dependence $P_x \propto \nu_{dr}^{-1}$ explains the well-known observational phenomenon that the power of the X-ray variability decreases when the source evolves to softer states. The resulting PDS continuum is a sum of two components, a low frequency (LF) component which presumably originates in an extended accretion disk and a high frequency (HF) component which originates in the innermost part of the source [Compton cloud (CC)]. The LF PDS component has a power-law shape with index of $1.0-1.5$ at higher frequencies ("red" noise) and a flat spectrum below a characteristic (break) frequency ("white" noise). This white-red noise (WRN) continuum spectrum holds information about the physical parameters of the bounded extended medium, diffusion time scale and the dependence law of viscosity vs radius. This LF PDS associated with the extended disk dominates in the soft states of the system, while the HF PDS characteristic of innermost CC component is dominant in the low/hard and intermediate states. These PDS LF and HF components directly correspond to the energy spectrum components. Namely: LF WRN is related to thermal emission from an accretion disk, and the HF WRN to the power-law tail, which presents a fraction of the disk emission Comptonized in the Compton cloud. Hence, a change of PDS features correlates with a change of energy spectral features. Analyzing the data for a number of sources we find that the PDS is well represented by a sum of the WRN CC component and the WRN extended disk component. We apply our model of the PDS to a sample of RXTE and EXOSAT timing data from Cyg X-1 and Cyg X-2 which describes adequately the spectral transitions in these sources.

Key words: accretion, accretion disks—black hole physics—stars:individual (Cyg X-1), individual (Cyg X-2) : radiation mechanisms: nonthermal—physical data and processes.

1. INTRODUCTION

In Astronomy, in general the basic question is: what one can learn from the observations confronting a theory derived from the first principles and the main laws of Physics. Particularly, X-ray Astronomy studies the spectral and timing properties of X-ray emission sources. During the last three decades a bulk of observational evidence emerged, showing that black hole X-ray binaries evolves through a set of spectral states [see 7, and references therein]. The basic properties of the X-ray energy spectra in a particular state are determined by a distribution of photons between two major spectral continuum components, i.e. the thermal component which comes from an accretion disk and the power law, presumably formed by the soft disk photons upscattered in a hot plasma surrounding the disk [Compton cloud (CC)]. Specifically, in the low-hard state the energy spectrum of a source is dominated by a power law part, while in high-soft states the thermal disk component is dominant. The Fourier Power Density Spectrum (PDS) also has a specific shape in each state. In low-hard state the source emission is highly variable (up to 40% root-mean-square (rms) variability) and PDS has a broken power law shape

with a flat plateau below the break frequency. In a less variable (less than 10 % rms) high-soft state PDS is a power law with index of 1.0-1.5 extending up to an orbital frequency of a binary system [1, hereafter GA07] with a cut-off at the higher frequencies. Many efforts have been made to build a consistent theory of PDS formation in accreting sources (see references below). In this Paper we present a model which is based on the exact analytical solution of perturbation diffusion equation in a bounded configuration (i.e. accretion disk or CC). The model explains the continuum shape of the observed PDS components as well as additional effects such as high frequency cut-off and rms-flux relationship [14].

King et al. [3] proposed an explicit physical model for the disc variability, consistent with Lyubarskii's general scheme [4], for solving this problem. They suggested that local dynamo processes can affect the evolution of the accretion disc by driving angular momentum loss in the form of an outflow (wind or jet). K04 argued that large-scale outflow can only occur when the small-scale random processes in neighboring disk annuli give rise by chance to a coherent large-scale magnetic field. This occurs on much longer time-scales (than that of the small-scale random processes), and causes a bright large-amplitude flare as a wide range of disc radii evolves in a coherent fashion. Most of the time, dynamo action instead produces small-amplitude flickering.

Lyubarskii [4] considered small amplitude local fluctuations in the accretion rate at each radius, caused by small amplitude variations in the viscosity, and then considers the effect of these fluctuations on the accretion rate at the inner disc edge. A linear calculation shows that if the characteristic time-scale of the viscosity variations is everywhere comparable to the viscous (inflow) time-scale, and if the amplitude of the variations is independent of radius, then the power spectrum of luminosity fluctuations is a power-law $1/\nu$. If the amplitude of the variations increases with radius, the slope of the power spectrum of the luminosity variations is steeper than 1. Lyubarskii pointed out that he had no physical model for the cause of such fluctuations. In particular, although the obvious candidate cause is the magnetic dynamo, the characteristic time-scales for the dynamo are much shorter than the local viscous time-scale.

In this Paper we present the exact treatment of the perturbation diffusion with the generic assumption regarding the disk viscosity, perturbation variability and its distribution in the disk. We apply the results of our theoretical investigations to the RXTE and EXOSAT observations of Cyg X-1 and Cyg X-2.

Gilfanov & Arefiev [1] analyzed the PDSs for a number of NS and BH sources using RXTE and EXOSAT observations in the wide frequency range, from 10^{-8} Hz to 10^{2} Hz. Particularly, they found the composite PDS of Cyg X-2. We reproduce their composite PDS. Furthermore, we infer the physical characteristics of the accretion flow in Cyg X-2 by application of our theory to the observable PDS.

2. EVOLUTION OF THE POWER SPECTRA. THEORETICAL CONSIDERATION

In this Paper we study the diffusive propagation of the local dynamical perturbations (fluctuations) in the disk-like bounded configuration. In other words, we assume that there is a temporal source of fluctuation at any point (radius) of the medium (disk) $\Phi(R,t)$. The X-ray time response of the disk, the luminosity perturbation, $\Delta L_x(t)$ can be considered in terms of diffusive propagation of the local driving perturbations $\Phi(R,t)$ in the disk. We assume that the temporal local variations of the mass supply in the disk around the steady state are small. They are only some fraction of the steady state mass supply through the disk. In other words, the amplitude of $\Phi(R,t)$ is proportional to the steady state mass accretion rate. Wood et al. [15], hereafter W01, show (see Eq. 7 there) that the mass accretion rate at the innermost radius of the disk $\dot{M}(R_{in},t)$ is proportional to the mass supply over the disk $A(t)$. It implies that the $\dot{M}(R_{in},t)$ perturbations, $\Delta\dot{M}(R_{in},t)$, should be proportional to $\Delta A(t) = 2\pi\int\Phi(R,t)RdR$ and consequently proportional to $A(t)$ because $\Delta A(t) \propto A$.

Thus one can formulate the problem of the diffusive propagation of the surface density perturbations $\Phi(R,t)$ in the bounded configuration (see Eq. 2 and Eq. 5 in W01). It is important to emphasize that this diffusive propagation of fluctuations (see Eq. 2) is an intrinsic property of a given disk-like configuration (necessary condition) where the angular momentum is distributed by diffusion.

The resulting power spectrum as a result of the diffusion of perturbations in the disk $||F_x(\omega)||^2$ is a product of the power spectrum of the temporal variation of source perturbations $||F_\varphi(\omega)||^2$ and the power spectrum of the disk response to the spatial distribution of the driving perturbations over the disk $||F_Y(\omega)||^2$ (see Eq. 18). Because the power of the driving perturbations $||F_\varphi(\omega)||^2$ is directly related to *the mass supply over the disk* $A(t)$ (see above) the intrinsic property of the diffusive propagation of the driving perturbation is *the existence of a strong relationship between the amplitude of the X-ray variability, related to* $||F_x(\omega)||^2$*, and the X-ray flux* $\propto A(t)$ [compare with the result of [14]].

If two disk-like bounded configurations are sources of the perturbation, i.e., $\Delta L_{x,1}(t)$ and $\Delta L_{x,2}(t)$ in the system which are weakly correlated, then the resulting power spectrum is a sum of the corresponding spectra (see Appendix A in [12], hereafter TSA07)

$$||F_x(\omega)|| \approx ||F_{x,1}(\omega)||^2 + ||F_{x,2}(\omega)||^2. \qquad (1)$$

2.1. Diffusive propagation of the perturbation in the disk. Formulation of the problem

Here we consider the diffusive propagation when the driving perturbations can be presented in a factorized

form $\Phi(t,R)=\varphi(t)f(R)$. In other words a spatial distribution of the driving perturbations in the disk is described by $f(R)$ and $\varphi(t)$ characterizes the perturbation input rate at any disk radius. In TSA07, Appendix B.1 we show that the diffusion solution for the general case of the function $\Phi(t,R)$ can be well approximated by the solution for $\Phi(t,R)=\varphi(t)f(R)$.

The diffusion equation for the time variable quantity $W(R,t)$, related to the surface density perturbations $\Delta\Sigma(R,t)$, $W(R,t)=\Delta\Sigma(R,t)$, can be written in an operator form (see Eq. 5 in W01):

$$\frac{\partial W}{\partial t}=\mathbf{\Lambda_R}W+\varphi(t)f(R) \qquad (2)$$

where R is a radial coordinate in the disk and $\mathbf{\Lambda_R}$ is the space diffusion operator. Equation (2) should be combined with the appropriate boundary conditions at $R=0$, $R=R_0$ and initial conditions at $t=0$. For homogeneous initial conditions, namely for $W(R,0)=0$ the solution at any R and t can be presented as a convolution

$$W(R,t)=\int_0^t\varphi(t')X(R,t-t')dt'. \qquad (3)$$

The kernel of convolution (3), $X(R,t-t')$ is a solution of the initial value problem for the homogeneous equation

$$\frac{\partial X}{\partial t}=\mathbf{\Lambda_R}X \qquad (4)$$

with the following initial conditions

$$X(R,t-t')_{t=t'}=X(R,0)=f(R) \qquad (5)$$

and with the same boundary conditions as that for $W(R,t)$ (we specify them in TSA07, §3, see also Eqs. 15, 16 in W01). The validity of $W(R,t)$, presented by formula (3), as a solution of Eq. (2) with the homogeneous initial condition can be directly checked by its substitution to Eq. (2) having in mind Eqs (4-5) for $X(R,t-t')$.

It is important to point out that the resulting perturbation signal is a sum of two components where one component is presented by formula (3) and another component is a solution of the initial value problem of a homogeneous diffusion equation, analogous to Eqs (4-5) but with the initial perturbation function that can be different from $f(R)$ (see TSA07, §3).

If the observational time intervals are much longer than the characteristic diffusion time scale of the perturbation in the disk t_0 then the contribution of the second component of the resulting signal is exponentially small. The amplitude of perturbations determined by the solution of the homogeneous problem [see Eqs (4-5)] decays exponentially for $t\gg t_0$ (see details in TSA07, §3).

The power spectrum $||F_W(\omega)||^2$ of $W(R,t)$ can be presented as a product of the power spectra $||F_\varphi(\omega)||^2$ and $||F_X(\omega)||^2$ of $\varphi(t)$ and $X(R,t)$ respectively:

$$||F_W(\omega,R)||^2=||F_\varphi(\omega)||^2||F_X(\omega,R)||^2 \qquad (6)$$

where $F_W(\omega,R)$, $F_\varphi(\omega)$, $F_X(\omega,R)$ are Fourier transforms of $W(R,t)$, $\varphi(t)$, $X(R,t)$ respectively.

The X-ray resulting variable signal is determined by the fluctuations of the luminosity $\Delta L_x(t)$. We assume that the mass accretion rate variations $\Delta\dot{M}(0,t)$ is converted with efficiency ε_{eff} into the variations of the X-ray luminosity, i.e. $\Delta L_x(t)=\varepsilon_{eff}\Delta\dot{M}(0,t)$.

W01 show that for the function $\mathcal{W}(x,t)=x\hat{\nu}W(x^2,t)$ using a new variable $x=R^{1/2}$ the diffusion equation (2) can be presented in the form

$$\frac{\partial\mathcal{W}}{\partial t}=\frac{3\hat{\nu}(x)}{4x^2}\frac{\partial^2\mathcal{W}}{\partial x^2}+\varphi(t)\mathcal{F}(x) \qquad (7)$$

where $\hat{\nu}(x)$ is viscosity in the disk, $\mathcal{F}(x)=x\hat{\nu}(x)f(x^2)$. The convolution, similar to Eq. (3), presents the solution $\mathcal{W}(x,t)$

$$\mathcal{W}(x,t)=\int_0^t\varphi(t')\mathcal{X}(x,t-t')dt' \qquad (8)$$

where $\mathcal{X}(x,t)$ is a solution of the initial value problem (compare with Eqs. 4, 5)

$$\frac{\partial\mathcal{X}}{\partial t}=\frac{3\hat{\nu}(x)}{4x^2}\frac{\partial^2\mathcal{X}}{\partial x^2} \qquad (9)$$

with the following initial conditions

$$\mathcal{X}(x,0)=\mathcal{F}(x). \qquad (10)$$

W01 (see Eq. 10 there) find that

$$\Delta L_x(t)=\varepsilon_{eff}\Delta\dot{M}(0,t)=3\pi\varepsilon_{eff}\frac{\partial\mathcal{W}}{\partial x}(0,t). \qquad (11)$$

The total X-ray deposition of the fluctuations at the inner disk edge Q_x can be obtained if we integrate Eq. (7) over t (from 0 to ∞) and over x (from 0 to $x_0=R_0^{1/2}$). Note that the time integral in the left hand side of Eq. (7)

$$\int_0^\infty\frac{\partial\mathcal{W}}{\partial t}dt=\mathcal{W}(x,t)|_{t=\infty}-\mathcal{W}(x,t)|_{t=0}=0 \qquad (12)$$

because we are only interested in the solution for which $\mathcal{W}(x,\infty)=\mathcal{W}(x,0)=0$. Thus using the integration of the right hand side of (7) combined with Eq. (11) and the outer boundary condition $\partial\mathcal{W}/\partial x(x_0,t)=0$ (see W01, Eq. 15) and keeping in mind the relation $x=r^{1/2}$ we find that

$$Q_x=\int_0^\infty\Delta L_x(t)dt=$$

$$\left[\varepsilon_{eff}\int_0^{R_0}f(R)2\pi RdR\right]\int_0^\infty\varphi(t)dt=C_{dr}\int_0^\infty\varphi(t)dt. \qquad (13)$$

Since the function $f(R)$ determines the shape of the spatial distribution of the driving perturbation only, we can

normalize $f(R)$ in such a way that the factor C_{dr} in the right hand side of Eq. (13) is equal to 1, namely

$$C_{dr} = \varepsilon_{eff} \int_0^{R_0} f(R) 2\pi R dR = 1. \qquad (14)$$

In this case the total X-ray fluctuation energy Q_x is equal to the integrated input (flux) of the driving perturbations over the disk:

$$Q_x = \int_0^{\infty} \varphi(t) dt = Q_{dr}. \qquad (15)$$

Eq. (15) implies that the emergent variable flux of X-ray emission Q_x is the same as the integrated input of the driving perturbations over the disk Q_{dr}. In other words *the driving perturbation flux is conserved when the perturbations diffuse through the disk towards the inner disk edge*.

On the other hand *the integrated power of the resulting PDS P_x is only a small fraction of the integrated power of the driving oscillations, P_{dr}, distributed over the disk*. The ratio P_x/P_{dr} strongly depends on the diffusion timescale in the disk t_0 and on the characteristic frequency of the driving oscillations ν_{dr} [$\nu_{dr} = \omega_{dr}/(2\pi)$].

In fact, the resulting X-ray signal due to the diffusion of the driving perturbations is

$$\Delta L_x(t) = \int_0^t \varphi(t') Y(t - t') dt', \qquad (16)$$

$$Y(t) = 3\pi\varepsilon_{eff} \frac{\partial \mathcal{X}(0, t - t')}{\partial x}. \qquad (17)$$

To obtain Eqs. (16) and (17) we use Eqs. (8) and (11).

Then the resulting power spectrum is

$$||F_x(\omega)||^2 = ||F_\varphi(\omega)||^2 ||F_Y(\omega)||^2 \qquad (18)$$

where $F_x(\omega),\ F_\varphi(\omega),\ F_Y(\omega)$ are Fourier transforms of $\Delta L_x(t),\ \varphi(t),\ Y(t)$ respectively [see e.g. TSA07, Eq. (7) for definition of the Fourier transform].

The disk local driving oscillations convolved with the response of the disk-like configuration results in the emergent response of the system $\Delta L_x(t)$. Ultimately, the power spectrum $||F_x(\omega||^2$ of $\Delta L_x(t)$ carries the information on the characteristic frequencies and the hydrodynamical structure of the system.

In general, the disk driving fluctuation $\varphi(t)$ can be presented as damped quasi-periodic oscillations for which power spectrum is Lorentzian

$$||F_\varphi(\omega)||^2 \propto [(\omega - \omega_{dr})^2 + (\Gamma_{dr}/2)^2]^{-1} \qquad (19)$$

where Γ_{dr} is a damping factor. We suggest that the frequency of the disk driving oscillations ω_{dr} (as a frequency of the Raylegh-Taylor gravity waves) is scaled with the local Keplerian frequency $\omega_{\rm K}$. In fact, ω_{dr} is some mean value of the rotational frequency of the local quasiperiodic oscillations in the disk-like configuration (see TSA07, Appendix B.1).

Now we proceed with an estimate of the integrated total power of the resulting signal $P_x = \int_0^\infty ||F_x(\omega)||^2 d\omega$. Using a relation Eqs. (18), and Eqs. (B15, B18, B19) in TSA07 we obtain that the integrated total power of the resulting signal

$$P_x = \int_0^{\infty} ||F_x(\omega)||^2 d\omega \sim \frac{1}{D\mathcal{Q}} \frac{P_{dr}}{\omega_{dr} t_0}. \qquad (20)$$

Here $\mathcal{Q} = \omega_{dr}/\Delta\omega \gtrsim 1$ stands for a quality factor, as $\Delta\omega$ stands for a FWHM of $||F_\varphi(\omega)||^2$ and a numerical factor $D \gtrsim 1$. We emphasize that $\omega_{dr} t_0 \gg 1$ because the diffusion time scale in the disk t_0 is likely much longer than the timescale of (local) driving oscillation $t_{dr} \sim \omega_{dr}^{-1}$.

Thus using equation (20) we arrive to the conclusion that the *resulting integrated power P_x, which is related to the perturbation amplitude at the inner disk edge, is much less than the total integrated power of the driving oscillation in the disk P_{dr}*

$$\frac{P_x}{P_{dr}} \sim (D\mathcal{Q}\omega_{dr} t_0)^{-1} \ll 1. \qquad (21)$$

This is a prediction of our diffusion model. The model can be confirmed or refuted if one can determine product of ω_{dr} and t_0 from observations and compare this with the observed ratio of P_x and P_{dr}. In TSA07, §5 we demonstrate the validity of our model using the power spectrum of Cyg X-1 obtained in the broad frequency range, from 10^{-7} Hz to 10^2 Hz.

Even though the specific mechanism providing the disk viscosity needs to be understood, the diffusion time scale in the disk and driving oscillation frequency "control" the variability of the innermost region of the accretion disk (Compton cloud). As seen from Eq. (21) the power (rms^2) of the resulting disk fluctuations should decrease with ω_{dr}. On the other hand it is well established (see e.g. ST06) that the X-ray emission area (Compton cloud) becomes more compact when the X-ray source evolves from hard to soft states. Average driving oscillation frequency ω_{dr} should progress to higher values during this evolution because it is scaled with some mean $\omega_{\rm K}$ over the Compton cloud. Probably this dependence of P_x with ω_{dr} is a key to explain the rms decay when the X-ray source evolves from hard to soft states, and when ω_{dr} increases (see more details of this effect in coming paper by Titarchuk & Shaposhnikov 2007).

3. DIFFUSION OF THE RADIAL LOCAL PERTURBATIONS IN THE DISK AS AN ORIGIN OF THE "WHITE-RED" NOISE

The diffusive propagation of the perturbation in the disk was studied by W01 in detail. They presented the diffusion equation for the surface density $\Sigma(R, t)$ as a function

of time t and the radial position in the disk R (see Eq. 5 in W01). It is worth noting that the derived equation is valid for any disk-like configuration for which the rotational frequency profile is Keplerian. This configuration can be a Shakura-Sunyaev type of disk [8] or an advection dominated accretion flow ([5], [2]). Thus this applies to the Compton cloud as well.

It is also important to emphasize that the equation derived for the surface density can be used as an equation for the surface density perturbations $\Delta\Sigma(R,t)$ in framework of the linear perturbation theory (see also §2.1).

In section §2 *we demonstrated that the determination of the diffusion response of the disk to the driving oscillations $\varphi(t)f(R)$ is reduced to the convolution of $\varphi(t)$ with the solution of the initial value (Cauchy) problem $Y(R,t)$ for the distributed perturbations at the initial moment $f(R)$* [see Eqs. (4, 5)]. Furthermore we show that the resulting power spectrum $||F_x(\omega)||^2$ is a product of power spectra $||F_\varphi(\omega)||^2$ and $||F_Y(\omega)||^2$ of $\varphi(t)$ and $Y(R,t)$ respectively (see Eq. 18).

In TSA07 we showed that for a linear dependence of the viscosity $\hat{\nu}(R)$ on R and a quasi-uniform distribution of the source perturbations the power spectrum $||F_Y(\omega)||^2$ can be presented by an exact analytical formula {see [6], formulas 5.1.28.1}. Thus

$$||F_Y(\nu)||^2_\nu \propto \frac{\pi}{2^{3/2}a^{3/2}}\frac{\sinh 2^{1/2}\pi a^{1/2}+\sin 2^{1/2}\pi a^{1/2}}{\cosh 2^{1/2}\pi a^{1/2}-\cos 2^{1/2}\pi a^{1/2}}- \\ -\frac{\pi}{2^{5/2}a^{3/2}}\frac{\sinh \pi a^{1/2}/2^{1/2}+\sin \pi a^{1/2}/2^{1/2}}{\cosh \pi a^{1/2}/2^{1/2}-\cos \pi a^{1/2}/2^{1/2}} \quad (22)$$

where $a = 8t_0\nu/\pi$ and $t_0 = 4R_0^2/3\hat{\nu}(R_0)$. t_0 is the viscous timescale and determines both the rise and fall time of the response function $Y(t)$ (see details in W01). As it follows from this formula that

$$||F_Y(\nu)||^2_\nu = C_N \times \pi^4/96 \quad \text{when} \quad \nu \ll \pi/8t_0 \quad (23)$$

and

$$||F_Y(\nu)||^2_\nu = C_N \times \frac{1}{2^7\pi^{1/2}t_0^{3/2}}\frac{1}{\nu^{3/2}} \quad \text{when} \quad \nu \gg \pi/8t_0. \quad (24)$$

TSA07 also found the behavior of the power spectrum in the case of arbitrary disk viscosity as a function of R, namely for $\hat{\nu}(R) \propto R^{\psi/2}$. We have already demonstrated for the $\psi = 2$ (linear) case that the power spectrum is a constant (the white noise) at very low frequencies ($\nu \ll \pi/8t_0$) and the power law with index $3/2$ at high frequencies $\nu \gg \pi/8t_0$ (so called the "red" noise). TSA07 showed that the white-red noise (WRN) power spectrum for the $\psi = 2$ case is presented as a series. The calculation of the series is reduced to analytical formula (22) from which low and high-frequency asymptotes are evident (see formulas 23, 24).

The similar presentation and asymptotic form of the power spectrum can be obtained in a general case of the disk viscosity i.e. for any ψ. Although the series of power spectrum

$$||F_Y(\nu)||^2_\nu \propto \\ \sum_{k=1}^{\infty}\frac{[2k-(10-3\psi)/2(4-\psi)-\varepsilon_k/\pi]^{2\delta}}{(8t_0\nu/\pi)^2+[2k-(10-3\psi)/2(4-\psi)-\varepsilon_k/\pi]^4} \quad (25)$$

has to be calculated numerically [a reader can find formula for ε_k in TSA07 (Eq. 60)] the asymptotic forms of $||F_Y(\nu)||^2_\nu$ can be easily evaluated analytically:

$$||F_Y(\nu)||^2_\nu = C_N \times \mathcal{A}_L \quad \text{when} \quad \nu \ll \pi/8t_0 \quad (26)$$

and

$$||F_Y(\nu)||^2_\nu = C_N \times \frac{\mathcal{A}_H}{\nu^{(3-2\delta)/2}} \quad \text{when} \quad \nu \gg \pi/8t_0 \quad (27)$$

where

$$\mathcal{A}_L = \sum_{k=1}^{\infty}\frac{1}{[2k-(10-3\psi)/2(4-\psi)-\varepsilon_k/\pi]^{4-2\delta}}, \quad (28)$$

$$\mathcal{A}_H = \frac{1}{2(8t_0\pi)^{(3-2\delta)/2}}\int_{x_1(\nu)}^{\infty}\frac{x^\delta dx}{1+x^4}, \quad (29)$$

$$x_1(\nu) = \frac{2t_0^{1/2}\lambda_1/\pi}{(8t_0\nu/\pi)^{1/2}} \quad (30)$$

and $\delta = (\psi-2)/(4-\psi)$. Thus using this formula for δ and Eqs. (27, 29, 30) we obtain the index of the power-law part of the power spectrum for a given ψ:

$$\alpha = \frac{3}{2}-\delta = \frac{16-5\psi}{2(4-\psi)} \quad \text{for} \quad \psi > 0$$

and

$$\alpha = 2 \quad \text{for} \quad \psi < 0. \quad (31)$$

In Figure 1 we show the example of white-red noise (WRN) PDS calculated using formula (25) for $\psi = 2$. One can clearly see the low-frequency asymptotic form (white-noise shoulder) and high-frequency asymptotic form (red-noise power law with index 3/2, see Eqs 26-27) there. For comparison we also show the PDS of an exponential shot which has a Lorentzian shape and PDS for the fast rise exponential decay (FRED) signal (see a formula for the FRED PDS in TSA07, Eq.76).

4. APPLICATIONS OF THE THEORY TO CYG X-1 AND CYG X-2 DATA

We now apply the PDS diffusion model to a data sample from the well-studied black hole X-ray binary Cyg X-1. The sample includes observations for all spectral states, from low-hard to high-soft states. An identification number of each RXTE observation of this sample is presented in Table 1 of TSA07. We also show a data sample for Cyg X-2 which is a neutron star (NS) source. Cyg X-2 was always in the high/soft state during RXTE and EXOSAT observations.

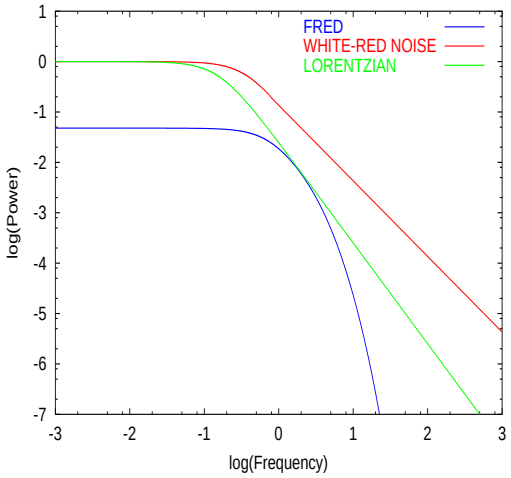

Figure 1. Examples of PDS models: PDS of white-red noise (red line), Lorentzian PDS (green line) and FRED PDS (blue line).

For our analysis we used Cyg X-1 and Cyg X-2 data from the Proportional Counter Array (PCA) and All-Sky Monitor (ASM) onboard *RXTE* [11] and the medium energy (ME) detector of the EXOSAT satellite [13]. The data are available through the GSFC public archive [1]. A reader can find the details of Cyg X-1 observations during the entire *RXTE* era in [9], hereafter ST06. These data cover the period 1996 - 2006 (MJD range $\sim$ 50100 - 53800).

It is known that Cyg X-1 often performs state transition from regular low/hard state to rarer soft state and vice versa (see ST06 for more details of Cyg X-1 spectral state history). To avoid the influence of such transitions on the composite EXOSAT-ASM power spectrum we have separately calculated PDS for low/hard and soft states of Cyg X-1. To identify a spectral state we have calculated the power-law index of the photon spectrum Γ based on ASM data from different energy channels [10]. For low/hard state we have collected individual dwell measurements with $\Gamma < 1.5$. For soft state we have chosen observations with $\Gamma > 2.5$ from 2002 year only. This period was uniquely long when Cyg X-1 stayed most of the time in the soft state.

We also employ a similar procedure to find the appropriate high-frequency (PCA) part of a broadband PDS. Namely, we identify a group of PCA observations by photon spectral index, i.e. observations in a similar spectral state and choose the one with PDS low-frequency part most closely matching the appropriate high-frequency part of EXOSAT PDS where they overlap. Our theoretical model reproduces the observable PDS shape of Cyg X-1 down to low frequencies (see Fig. 2 - 3). In the low-hard and high-soft states the power spectrum continuum is fitted by our diffusion model. However, one or two relatively broad Lorentzians are needed for fitting of QPO features observed in the low-hard and intermediate states of Cyg X-1.

[1] http://heasarc.gsfc.nasa.gov

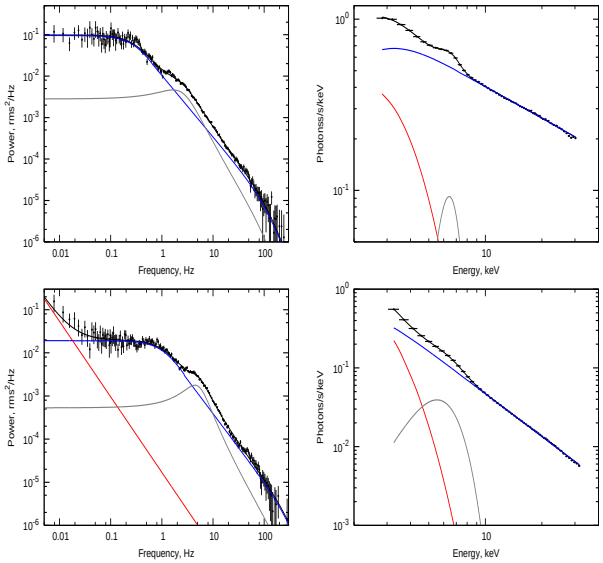

Figure 2. Cyg X-1: Observable power spectrum (PDS) (left panel) vs photon spectrum (right panel). The first observation is a pure low/hard state with no LF WRN component in the PDS. During the second observation the source energy spectrum is still hard, but LF WRN is already detectable. PDS is fitted by a sum of LF and HF WRN power spectra We also use Lorentzians to fit QPO features. Black line is for the resulting PDS as red and blue lines present LF and HF components respectively. Photon spectrum is fitted by BMC+GAUSSIAN model, where BMC stands for the bulk motion Comptonization model in XSPEC. The resulting model spectrum is shown in black, while red and blue curves present thermal and Comptonized components respectively.

We clearly see two independent hydrodynamical components in the accretion flow. Their presence are confirmed by power and photon spectra. They are presumably related to an extended Keplerian disk [8] and a compact geometricaly thick sub-Keplerian halo-Compton cloud (see [2], [5]). In Figures 2 and 3 we present the observable evolution of RXTE/PCA PDS and photon spectra of Cyg X-1. PDS is fitted a sum of LF and HF WRN power spectra and a zero-centered Lorentzian plus the narrow Lorentzians to fit QPO features. This model is consistent with the data. We use ASM and EXOSAT data in order to extend the PCA PDSs presented in Figs. 2-3 to much lower frequencies. In Figure 4 we show two composite EXOSAT/PCA PDSs of Cyg X-1 for the low/hard state. For presentation purposes the upper PDSs are multiplied by additional factors of 10^3.

It is worth noting that *the low frequency power-law slope is either barely observed or not observed at all in PCA data alone at low/hard state from 0.01 Hz to 100 Hz (Figs. 2, 3) but it can be clearly seen at longer time scales, probed with EXOSAT.*

Thus, EXOSAT observes the presence of low frequency power slope related to LF part of our model along with the presence of high frequency power slope which is the

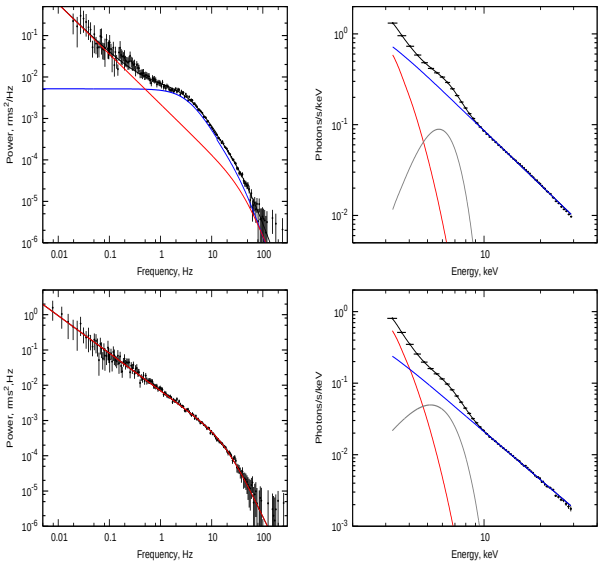

Figure 3. The same as Figure 2. The first observation (upper panel) is taken during the intermediate state just before the transition to high/soft state, which is presented by the second observation (lower panel). No HF WRN is present in PDS during high/soft state.

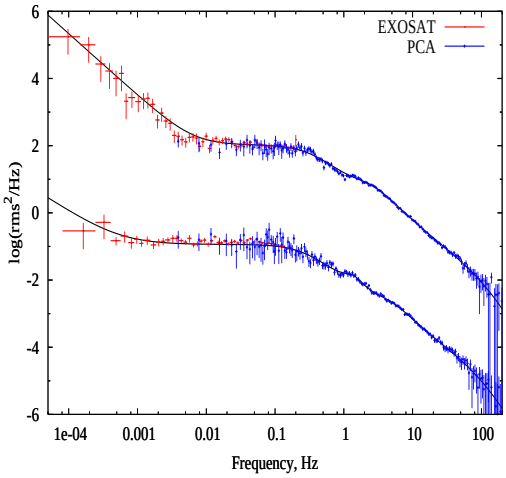

Figure 4. Two composite PDSs: EXOSAT spectra with matching high frequency PCA PDS. Data are fitted by LF-HF diffusion model: $\chi^2/N_{dof} = 250.1/267 = 0.94$, $\psi_{CC} = 2.32 \pm 0.12$, $t_{0,C} = 1.8 \pm 0.3$, $\psi_D = 2.5$ *(fixed) and* $\chi^2/N_{dof} = 278.5/267 = 1.04$, $\psi_{CC} = 2.07 \pm 0.7$, $t_{0,C} = 1.24 \pm 0.12$, $\psi_D = 0.3 \pm 0.3$ *(fixed) for lower and upper fits respectively.*

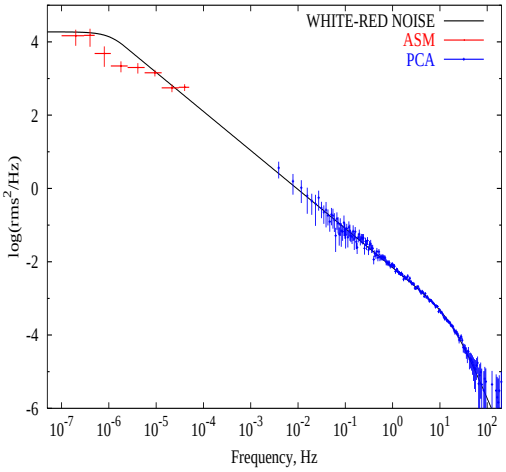

Figure 5. The composite soft state PDS is made by PCA (blue) and ASM (red) PDSs. Data are fitted by LF-HF diffusion model: $\chi^2/N_{dof} = 184/228 = 0.81$, *the best - fit parameters* $t_{0,D} = (6 \pm 1.7) \times 10^5$ *s,* $\psi_D = 2.93 \pm 0.01$.

HF part of our model. One can expect that low frequency and high frequency power-law slopes can always be observed in the power spectrum of low/hard state of Cyg X-1 if one could have simultaneously long observations with high timing resolution. ASM/PCA PDS of the high-soft state is shown on Figure 5.

The Composite Power Spectrum of Cyg X-2. We also constructed the composite PDS for a neutron star source Cyg X-2 using ASM-PCA of RXTE and EXOSAT data in Figure 6. Cyg X-2 is most of the time in high-soft state, when the photon spectral index is about 4 and higher. We found that the broadband PDS in Cyg X-2 has the structure similar to Cyg X-1. Namely, PDS consists of two (LF WRN and HF WRN) components. Presumably LF WRN and HF WRN components are related to the extended Keplerian disk and to relatively compact, inner disk-like configuration (sub-Keplerian Compton cloud which surrounds the neutron star) respectively. We fit Cyg X-2 PDS using our two components model. For the LF PDS component the best-fit parameters are: $t_{D,0} = (6.7 \pm 1) \times 10^5$ s, $\psi_D = 1.66 \pm 0.06$, and for the HF PDS component they are $t_{C,0} = 0.8056 \pm 0.0001$ s, $\psi_{CC} = 3.11 \pm 0.02$. QPO lowest frequency is $\nu_L = 60.03 \pm 2.25$ Hz.

5. THE MAIN RESULTS AND CONCLUSIONS

We conclude by summarizing the main results of the presented diffusion theory.

We have presented a detailed mathematical analysis of the perturbation diffusive propagation. We investigated the intrinsic properties of the disk density evolution equation (7) with the appropriate boundary and initial conditions in a general case. We have analyzed the diffusion

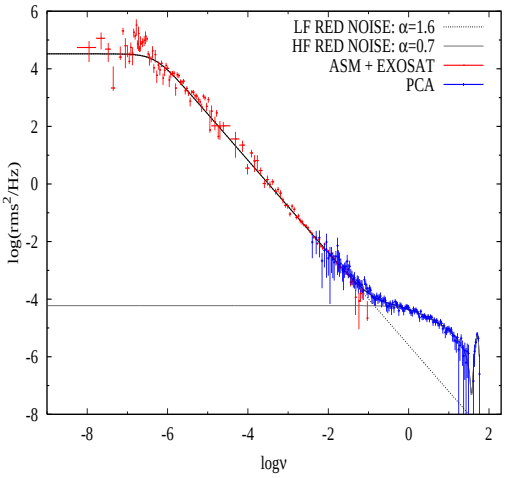

Figure 6. EXOSAT-ASM-PCA (RXTE) power spectrum of Cyg X-2 in frequency range that covers 10 orders of magnitude. One can clearly see low and high frequency (LF and HF) white-red noise components in PDS, related to the extended Keplerian disk and relatively compact, innner disk-like configuration (sub-Keplerian Compton cloud) respectively. Each of these two components is perfectly fitted by our white-red noise model, dotted and solid lines are for LF and HF best-fit models respectively, $\chi^2/N_{dof} = 393.2/244 = 1.6$ *(see the text for the best-fit parameters values).*

models determined by the disk viscosity dependence on the radius for various perturbation sources in the disk. We have examined the case where the viscosity is a power law function of position in the disk. Using the perturbations of the disk surface density $\Delta\Sigma(r,t)$ we are able to infer the evolution of the perturbations of the mass accretion rate in the inner disk edge and ultimately the perturbations of the X-ray luminosity as a function of time, $\Delta L_x(t)$. Then we calculate the power spectrum using the Fourier transforms of $\Delta L_x(t)$ and the driving perturbations. The PDS continuum (White-Red-Noise) is a power spectrum of the diffusion response of the disk-like configuration to the high frequency (local) driving disk oscillations. Whereas X-ray photon spectrum is the result of the soft photon diffusion upscattering (Comptonization) in the disk-like configuration (Compton cloud), the PDS is formed in the same configuration as a result of the diffusive propagation of high-frequency local driving perturbations. This solution is robust and generic.

The resulting model time signal as a linear combination of quite a few *related* exponential shots is in a good agreement with the observations. The observable PDS is perfectly fitted by a sum of LF and HF white-red noise power spectra. *This fact can be interpreted as an observational evidence of the presence of two independent components in the accretion flow.* One is related to the extended geometrically thin disk (LF PDS component) and the other - to the geometrically thick compact configuration (HF PDS component). Each of the white-red noise (WRN) components has two free parameters, the diffusion time scale t_0 and the viscosity index ψ. The value of the parameter t_0 has a physically plausible value for the viscous timescale of the disk-like configuration.

In the observed power spectra (particularly in the intermediate state) we deal with two diffusion time scales, one $t_{C,0}$ is related to the inner compact region, presumably Compton cloud (sub-Keplerian disk, ADAF) and the other $t_{D,0}$ is related to a much larger disk. The diffusion time scale of the inner region is scaled with the mass of the central object and $t_{D,0}$ is scaled with the orbital period of the system.

We present the broadband PDSs of the black hole source Cyg X-1 in hard (Fig. 4) and soft (Fig. 5) states, illustrating the presence of LF and HF components in hard state and the absence of HF component (or a weak HF) in the soft state. In Figures 2, 3 we show the evolution of LF and HF components in high frequency PDS of Cyg X-1. We also find that Cyg X-2 PDS also consists of LF and HF components (see Figure 6). The best-parameters of the model allows us to determine the diffusion time scales of geometrically thin extended disk $t_{D,0}$ and geometrically thick configuration (Compton cloud) $t_{C,0}$. They differ by almost six orders of magnitude, namely $t_{D,0} \sim 0.7 \times 10^6$ s and $t_{C,0} \sim 0.8$ s.

REFERENCES

[1] Gilfanov, M., & Arefiev, V. 2007, MNRAS, accepted, (astro-ph/0501215) (GA07)

[2] Chakrabarti, S.K. & Titarchuk, L. G. 1995, ApJ, 455, 623

[3] King, A.R., Pringle, J.E., West, R.G., & Livio, M. 2004, MNRAS, 348, 111 (K04)

[4] Lyubarskii, Yu., E. 1997, MNRAS, 292, 679 (L97)

[5] Narayan, R., & Yi, I. 1994, ApJ, 428, L13

[6] Prudnikov, A. P., Bruchkov, Yu. A., & Marichev, O. I. 1981, Integrals and Series (Moscow: Nauka) (PBM01)

[7] Remillard, R. A. & McClintock, J. E. 2006, ARA&A, 44, 49

[8] Shakura, N. I. & Sunyaev, R. A. 1973, A&A, 24, 337 (SS73)

[9] Shaposhnikov, N. & Titarchuk, L. 2006, ApJ, 643, 1098 (ST06)

[10] Smith, D. M., Heindl, W. A., & Swank, J. H. 2002, ApJ, 569, 362

[11] Swank, J. H. 1999, Nucl. Phys. B - Proc. Suppl., 69, 12, 569, 362

[12] Titarchuk, L., Shaposhnikov, N., & Arefiev, V. 2007, ApJ, 659, (astro-ph/0612675) (TSA07)

[13] Turner, M., Smith. A., & Zimmerman, H. 1981, Space Science Rev., 30, 513

[14] Uttley, P. 2004, MNRAS, 347, L61

[15] Wood, K. S., Titarchuk, L., Ray, P.S., et al. 2001, ApJ, 563, 246 (W01)